Autonomous Control of a Quadcopter via Fuzzy Gain Scheduled PD Control

Submitted by:

Saad Sardar

Supervised by:

Dr. Muhammad Bilal Kadri

THESIS

Submitted to:

Department of Electronic and Power Engineering

Pakistan Navy Engineering College Karachi

National University of Science and Technology, Islamabad Pakistan

In fulfillment of requirement for the award of the degree of

MASTER OF SCIENCE IN ELECTRICAL ENGINEERING

With Specialization in Control Engineering

Abstract

This thesis discusses the Intelligent Gain Scheduled PD technique to autonomously control the attitude of the Quad Copter. This thesis would focus on two aspects of the autonomous quadcopter i.e. Attitude Control and Trajectory Following. The autonomous control of a quad-copter is a challenge due to its non-linear dynamics and environmental perturbations. The environmental perturbations can easily tip off the stability of the quad-copter since it has coupled EOM (Equations of Motion) which makes it easier for a disturbance to mitigate the effects of one of the rotors to other three. The non-linear dynamics of the quad-copter aggressively diminishes the performance of PD furthermore the spontaneous switching of the rotors can burn their motors. The aim of the investigation is to study a Fuzzy Takagi-Sugeno method used to control the position and the yaw angle of the quad-copter. This investigation will be carried out using a complete Non-Linear Simulink model. We will discuss two control techniques i.e.

(i)   Gain Scheduled PD, with the

(ii)   Fuzzy Supervisory Gain Offset Mechanism/Capability to re-tune its parameters with the changing surroundings.

Adaptive Gain-Scheduled control is a combination of classical and modern control approaches. This technique keeps the onboard computational requirements very low while the adaptation process regularly update the gains to counter perturbations thus increasing the robustness of the overall system.

Acknowledgement

I am very much grateful to Almighty ALLAH, the most merciful and beneficent, whose ample blessings enable us to recognize and pursue knowledge in life. My sincere gratitude to my supervisor Dr. Muhammad Bilal Kadri, Assistant Professor, Department of Electronic and Power Engineering at PN Engineering College, NUST. I consider myself very lucky and honored to have him as my supervisor. I thank him for his unprecedented attention and patience throughout the thesis work. I admire him as a teacher and as a person.

In addition to above, I am also thankful to the guidance committee comprising of following faculty members who led me to achieve my target:

- Capt. Dr. Muhammad Junaid Khan TI(M) (PN)
- Cdr. Dr. Tariq Mairaj Khan(PN)
- Cdr. Dr. Ataullah Memon (PN)

I want to take this opportunity to thank my parents, my brothers and sister. Thank you for your prayers, love, encouragement, patience… Thank you for everything.

Table of Contents

List of Figures

List of Tables

List of symbols

a   lift slope

A   propeller disk area

A_c fuselage area

A_u Operational time (autonomy)

b   thrust factor

BW   propulsion group bandwidth

c   propeller chord

C   propulsion group cost factor

C_{bat} battery capacity

C_d drag coefficient at 70% radial station

C_H hub force coefficient

C_Q drag coefficient

C_{Rm} rolling moment coefficient

C_T thrust coefficient

d   drag factor

DoF   Degrees of Freedom

g   acceleration due to gravity

h   vertical distance: Propeller center to CoG

H   hub force

i   motor current

$I_{xx,yy,zz}$ inertia moments

J_m motor inertia

J_r rotor inertia

J_t total rotor inertia seen by the motor

k_e motor electrical constant

k_m motor torque constant

l   horizontal distance: propeller center to CoG

m   overall mass

m_{af}	airframe mass
m_{av}	avionics mass
m_{bat}	battery mass
m_{batav}	avionics' battery mass
m_{hel}	helicopter mass
m_{pg}	propulsion group mass
M_{BATmax}	maximum battery mass possible
$M_{maxpossible}$	maximum mass one motor can lift
$M_{maxrequested}$	requested mass for one motor to lift
n	number of propellers
P_{av}	avionics' power consumption
P_{el}	electrical power
P_{in}	gearbox input power
P_{out}	gearbox output power
Q	drag moment
Q_{pg}	propulsion group quality factor
Qin	design quality index
r	gearbox reduction ratio
R	rotation matrix
R_{rad}	rotor radius
R_{mot}	motor internal resistance
R_m	rolling moment
T	thrust force
T_w	propulsion group thrust/weight ratio
u	motor input
U	control inputs
V	body linear speed
x, y, z	position in body coordinate frame
X, Y, Z	position in earth coordinate frame

β	thrust/weight ratio
θ	pitch angle
v	speed vector
τ	motor time-constant

Chapter 1

Introduction

1.1. Background

A Quad-copter is a hot topic for research in the field of Civil and Defense Aerodynamic Research these days. Etienne Oehmichen in 1920's developed the first Quad-copter that was piloted by a human. Since then Aeronautical Engineers have been experimenting on that basic design and have finally arrived on a more feasible use i.e. a micro structured unmanned model that serves as a more stable and reliable platform for unmanned missions than its counterpart i.e. a helicopter.

They are a perfect apparatus for research into GNC (Guidance, Navigation and Control) and Real-time control systems for either a single or multiple vehicles.

It is used as an autonomous surveillance and sometimes as an independent security platform equipped with cameras and guns, it serves as in independent platform for a wide range of civil/commercial projects too. These machines are working alongside their human operators in projects that range from exploration to tracking, imaging (live feed) and SAR (Synthetic Aperture RADAR) platforms and even to explore Inhospitable Environments.

An advantage of rotating-wing over a fixed-wing aircraft is the ability to hover and a sideways maneuver. A drawback is however a relatively higher power consumption during the flight and the disability to glide in the event of actuator failure. However, a quad-copter is much simpler and easier to build since the rotational axes of its rotors are fixed and there are no moving parts such as aerodynamic control surfaces. Dynamically it is a highly unstable open loop system and that's what makes it a challenging control engineering problem.

1.2. Aim of Thesis

In this thesis we were given a special mission for our quadcopter design. The mission is to track a moving target on ground over a long period of time and to

report back the activity details of target to a ground station. The mission would comprise of following stages:

a) Takeoff and Land
b) Tracking the target.

Since the area in which the quad-copter would be deployed is a tropical jungle it would be impossible for a human on ground to navigate through a dense tree line and/or track a dangerous species.

All the above mentioned activities have to be fully autonomous since there is no expert human operator on ground.

1.3. Thesis Organization

The thesis is organized into five chapters as follows:

- Chapter 1 gives a brief introduction to this Research and its Aims and Objectives.
- Chapter 2 gives a Literature Review of the Navigational Frames of Reference used in this thesis.
- Chapter 3 covers the mathematical modeling of the quadcopter and a derived linear model for use in the Hardware Processing Board.
  - o Mathematical model of Overall system
    - Kinematics Model
    - Attitude Model
- Chapter 4 discusses the Fuzzy based PD gain scheduling control strategy implemented in Simulink®.
  - o Implementation of PD Controller with System
  - o Fuzzy GS PD Controller [Kinematic and Attitude]
- Chapter 5 gives the comparison between the simulation results of PD control vs the Fuzzy Adaptive control.
- Chapter 6 chalks out the conclusion.

Chapter 2

Literature Review

2.1. Designs in Literature

2.1.1. Design of Fuzzy gain scheduled PID controller for JC2SAT-FF Mission

The JC2SAT-FF (Japan Canada Joint Collaboration Satellites – Formation Flying) mission is a joint venture between JAXA (Japan Aerospace Exploration Agency) and CSA (Canadian Space Agency). It is a simple scientific demonstration mission designed to evaluate a simple design strategy for a Leader Follower Formation Flying Satellites. Using Reaction wheels as main actuators to control the attitude of the satellites designers implemented a Fuzzy Gain Scheduled PID Controller that updates the controller gain as per the requirements of the actuator to counter the differential drag control on the face of the satellite and to provide a longer target tracking for the payload.

2.1.2. Fault-Tolerant Fuzzy Gain-Scheduled PID for a Quadrotor Helicopter Testbed in the Presence of Actuator Faults

In this study the designers had implemented a Fuzzy gain scheduled PID control for a Quadcopter testbed. The quadcopter worked under the constraint of actuator failure, two different faults were discussed:

- Loss of control in all actuators
- Loss of control in a single actuator

The controllers were first simulated using MATLAB then an experimental simulation was conducted in which actual Quadrotor was mounted on a fixed testbed, the Quadrotor was commanded through PC to perform certain maneuvers with randomly

induced actuator faults, the control strategy was very effective to maneuver the quad without plunging it into gyro instability. [1]

2.1.3. Control of a quadcopter using Self-Tuning Fuzzy PID Controller

In this paper the modelling, simulation-based controller design and path planning of a quadrotor is discussed. An EKF based self-tuning Fuzzy PID control is proposed for the attitude control.to reduce the computational time a Dijkstra's algorithm is used for path planning in a closed and known environment filled with obstacles and/or boundaries. The Dijkstra algorithm helps avoid obstacle and find the shortest route from a given initial position to the final position. [2]

2.1.4. Fuzzy Gain Scheduling PID Control Design Based on Particle Swarm Optimization Method

PID Control via a Particle Swarm Optimization (PSO) technique is used to control the coarse and heading of the ship. Factors including gain margin and oscillation frequency are determined by Ziegler-Nichols method and then through PSO method gains are optimized to improve the performance of controlled system. [9]

2.2. Reference Frames

There are two reference frames used in this thesis. A brief description of each is given below.

2.2.1. North East Down (NED) Inertial Frame

The Z-axis of the NED is pointed vertically down towards Earth's surface, the velocity vector is aligned towards the cardinal East and the x-axis points towards the celestial north as represented in Figure 2.2.4.1.
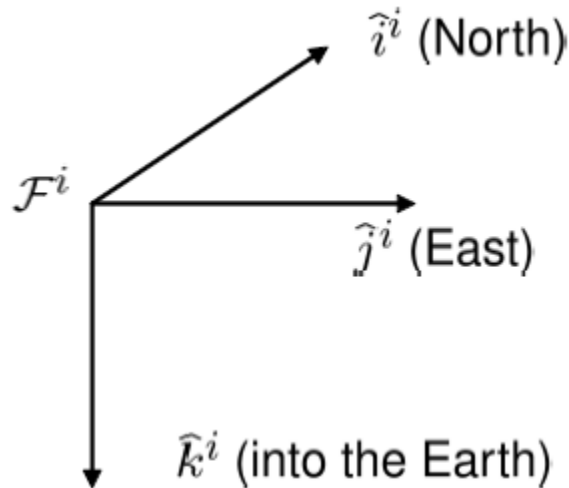
Figure 2.2.2.1-1 NED Frame

2.2.2. Body Axes Frame

As shown in figure 2.2.4.2 below the Body axes frame has its origin about the center of mass (CoM) of the quadcopter. The z axis of the system is pointing vertically downward representing the altitude of the system. The X axis is along rotors 1 and 2 and represents the forward movement of the quadcopter while the y axis is perpendicular to X and Z axes.
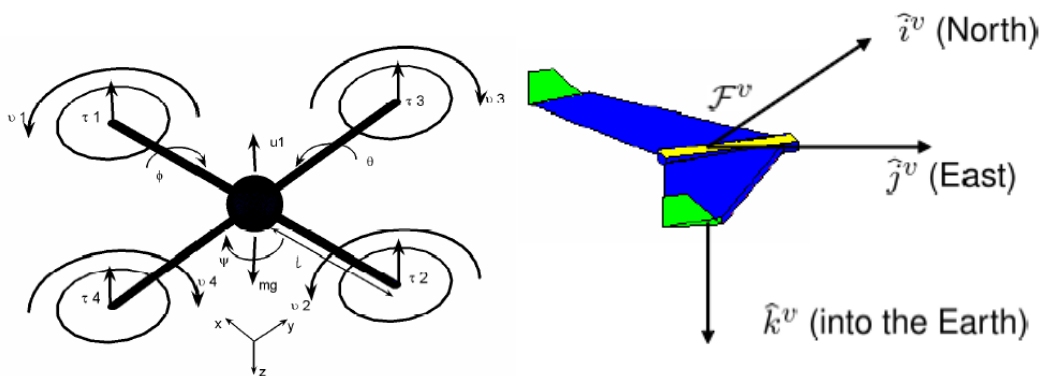

Figure 2.2.2.2-1 Body Frame

Rolling moment is about the Y axis of the body axis system, Pitch is about the X axis of the system and the Yaw is about the Z axis of the body frame. Respective thrusts can be mathematically mapped by the following equations:

$$\mu_{roll} = l(\mu_3 - \mu_4) \tag{3.1.1}$$

$$\mu_{pitch} = l(\mu_1 - \mu_2) \tag{3.1.2}$$

$$\mu_{yaw} = (\mu_1 + \mu_2 - \mu_3 - \mu_4) \tag{3.1.3}$$

Where;

$\mu_1, \mu_2, \mu_3 \ and \ \mu_4$ are the thrusts produced by the Motors 1, 2, 3 and 4 respectively.

2.3. Transformation Matrix

There is a need to formulate a transformation matrix that would translate the body coordinates into an Inertial Fixed Frame of reference i.e. N.E.D (North East Down) Frame counterparts. A 3x3 Rotation Matrix (DCM) is thus defined as follows:

$$R_{ned}^b = \begin{bmatrix} c_\varphi c_\theta & s_\emptyset s_\theta c_\varphi - c_\emptyset s_\varphi & c_\emptyset s_\theta c_\varphi + s_\emptyset s_\varphi \\ c_\theta s_\varphi & s_\emptyset s_\theta c_\varphi + c_\varphi c_\emptyset & c_\emptyset s_\theta c_\varphi - c_\varphi s_\emptyset \\ s_\theta & -c_\theta s_\emptyset & -c_\theta c_\emptyset \end{bmatrix} \tag{3.2.1}$$

Where:

- $\theta, \emptyset, \varphi$ are the roll, pitch and yaw angle respectively,
- $s_\theta = \sin(\theta), c_\theta = cos(\theta), s_\emptyset = sin(\emptyset), s_\varphi = \sin(\varphi)$ and so on.

Chapter 3

Kinematics and Dynamics

Derivation of Rigid body dynamics and kinematics equations of quadcopter will be discussed in detail in this chapter.

The following twelve states encompass the rotational dynamics and translational kinematics of the overall system:

- p_n defines the Inertial North position of the quadcopter in Inertial frame
- p_e defines the Inertial East position of the quadcopter in Inertial frame
- h defines the Inertial Vertical height of the quadcopter in Inertial frame
- u gives the body frame velocity vector along body x-axis
- v gives the body frame velocity vector along body y-axis
- w gives the body frame velocity vector along body z-axis
- $\emptyset$ is the Roll angle of system defined in body frame x-axis
- θ is the Pitch angle of system defined in body frame y-axis
- φ is the Yaw angle of system defined in body frame z-axis
- p denotes the roll rate along x-axis
- q denotes the pitch rate along y-axis
- r denotes the yaw rate along z-axis

3.1. Quadcopter Dynamics

The dynamics of the quadcopter are derived through Newton-Euler formulation.

Let v be the velocity of the rotor in inertial frame, then Newton's second law of motion states that;

$$m\,\dot{v} = f \qquad \text{Equation 3.1-1}$$

Where m is the mass of the overall system and **f** is the total force applied to the quadcopter.

Now introducing equation of Coriolis; we get:

$$m\,\dot{v} = m\left(\frac{dv}{dt_b} + \omega_{b/ned} \times v\right) = f \qquad \text{Equation 3.1-2}$$

where $\omega_{b/ned}$ is the system's angular velocity w.r.t inertial frame NED.

Eq(3.1-2) is the governing equation for system's dynamics in NED frame; however; the control force is computed in vehicle/body frame, so Eq(3.1-2) can be re-written in body frame using quantities 4-6 and 10-12 stated above.

$$\begin{pmatrix} \dot{u} \\ \dot{v} \\ \dot{w} \end{pmatrix} = \begin{pmatrix} rv - qw \\ pw - ru \\ qu - pv \end{pmatrix} + \frac{1}{m} \begin{pmatrix} f_x \\ f_y \\ f_z \end{pmatrix} \qquad \text{Equation 3.1-3}$$

Moving forward with rotational motion, the momentum transfer equation derived from Newton's second law states that:

$$\frac{dh^b}{dt} = m \qquad \text{Equation 3.1-4}$$

Where h is the total body momentum and m is the applied torque.

Again using the equation of Coriolis, above equation can be transformed into the following form:

$$\frac{dh}{dt_i} = \frac{dh}{dt_b} + w_{b/i} \times h = m \qquad \text{Equation 3.1-5}$$

The term h^b in Eq (3.1-3) in body coordinates is composed of the total inertia J and rotational velocity $w_{b/i}^b$; i.e.;

$$h^b = J w_{\frac{b}{i}}^b$$

Where $J = \begin{pmatrix} J_x & 0 & 0 \\ 0 & J_y & 0 \\ 0 & 0 & J_z \end{pmatrix}$; since it is assumed that the quadcopter has a symmetric mass distribution in xyz axes.

$$\begin{pmatrix} \dot{p} \\ \dot{q} \\ \dot{r} \end{pmatrix} = \begin{pmatrix} \frac{1}{J_x} & 0 & 0 \\ 0 & \frac{1}{J_y} & 0 \\ 0 & 0 & \frac{1}{J_z} \end{pmatrix} \left[\begin{pmatrix} 0 & r & -q \\ -r & 0 & p \\ q & -p & 0 \end{pmatrix} \begin{pmatrix} J_x & 0 & 0 \\ 0 & J_y & 0 \\ 0 & 0 & J_z \end{pmatrix} \begin{pmatrix} p \\ q \\ r \end{pmatrix} + \begin{pmatrix} \tau_\phi \\ \tau_\theta \\ \tau_\varphi \end{pmatrix} \right]$$

$$= \begin{pmatrix} \frac{J_y - J_z}{J_x} qr \\ \frac{J_z - J_x}{J_y} pr \\ \frac{J_x - J_y}{J_z} pq \end{pmatrix} + \begin{pmatrix} \frac{1}{J_x} \tau_\emptyset \\ \frac{1}{J_y} \tau_\theta \\ \frac{1}{J_z} \tau_\varphi \end{pmatrix} \qquad \textbf{Equation 3.1-6}$$

3.2. Quadcopter Kinematics

The variables listed above as p_n, p_e and h are inertial frame quantities i.e. they are represented in NED frame as stated above whereas, the quantities *u, v and w* are their body frame counterparts. [6][7]

They are translated via a rotational matrix R_b^v as given in equation below:

$$\frac{d}{dt} \begin{pmatrix} p_n \\ p_e \\ -h \end{pmatrix} = (R_v^b)^T \begin{pmatrix} u \\ v \\ w \end{pmatrix}$$

$$= \begin{bmatrix} c_\varphi c_\theta & s_\emptyset s_\theta c_\varphi - c_\emptyset s_\varphi & c_\emptyset s_\theta c_\varphi + s_\emptyset s_\varphi \\ c_\theta s_\varphi & s_\emptyset s_\theta c_\varphi + c_\varphi c_\emptyset & c_\emptyset s_\theta c_\varphi - c_\varphi s_\emptyset \\ s_\theta & -c_\theta s_\emptyset & -c_\theta c_\emptyset \end{bmatrix} \begin{pmatrix} u \\ v \\ w \end{pmatrix} \qquad \textbf{Equation 3.2-1}$$

Most importantly we need to relate *p, q, r* to $\dot\emptyset, \dot\theta, \dot\varphi$. The relationship between them is given as follows:

$$\begin{pmatrix} p \\ q \\ r \end{pmatrix} = R_{v2}^b(\dot\emptyset) \begin{pmatrix} \dot\emptyset \\ 0 \\ 0 \end{pmatrix} + R_{v2}^b(\emptyset) R_{v1}^{v2}(\dot\theta) \begin{pmatrix} \dot\emptyset \\ 0 \\ 0 \end{pmatrix} + R_{v2}^b(\emptyset) R_{v1}^{v2}(\theta) R_{v \to v1}(\dot\varphi) \begin{pmatrix} \dot\emptyset \\ 0 \\ 0 \end{pmatrix}$$

$$= \begin{pmatrix} 1 & 0 & -s\theta \\ 0 & c\emptyset & s\emptyset c\theta \\ 0 & -s\emptyset & c\emptyset c\theta \end{pmatrix} \begin{pmatrix} \dot\emptyset \\ \dot\theta \\ \dot\varphi \end{pmatrix} \qquad \textbf{Equation 3.2-2}$$

3.3. Forces and Moments

Forces and torques acting on the quadcopter are described in this chapter. Due to the absence of aerodynamic lifting surfaces it is assumed that aerodynamic forces and moments are negligible. The main forces and moments are due to gravity and the four propellers. [6]
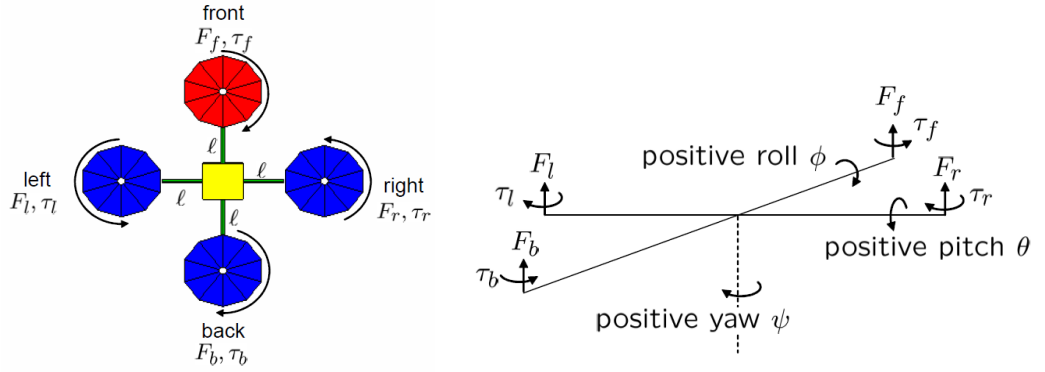
Figure 3.3-1 Top View of Quadcopter System

$$F = F_f + F_r + F_b + F_l$$

Equation 3.3-1

The rolling torque produced by the sum of forces on the right and left motors is given by:

$$\tau_\phi = l\,(F_l - F_r)$$

Equation 3.3-2

Similarly, the pitching torque is produced by the forces acting on the front and back motors is given as follows:

$$\tau_\theta = l\,(F_f - F_b)$$

Equation 3.3-3

Newton's third law of motion states that the propeller drag produces a counter torque on the quadcopter opposite to the direction of the motion of the propellers. Therefore the total yawing torque is given by:

$$\tau_\psi = \tau_r + \tau_l - \tau_f - \tau_b$$

Equation 3.3-4

The lift and drag i.e. produced by the propellers is proportional to the square of the angular velocity, assuming that the angular velocity is directly proportional to the pulse width modulation commend sent to the motor the force and torque of each motor can be expressed as [8]:

$$F_* = k_1\delta_*$$

Equation 3.3-5

$$\tau_* = k_2\delta_*$$

Equation 3.3-6

Where; k_1 and k_2 are constants needed to be determined experimentally, δ_* is the motor command signal, and $*$ represents *f, r, b, and l*. The forces and torques on the quadcopter can be written in matrix form as: [7]

20

$$\begin{pmatrix} F \\ \tau_\phi \\ \tau_\theta \\ \tau_\psi \end{pmatrix} = \begin{pmatrix} k_1 & k_1 & k_1 & k_1 \\ 0 & -lk_1 & 0 & lk_1 \\ lk_1 & 0 & -lk_1 & 0 \\ -k_2 & k_2 & -k_2 & k_2 \end{pmatrix} \begin{pmatrix} \delta_f \\ \delta_r \\ \delta_b \\ \delta_l \end{pmatrix} \triangleq \mathcal{M} \begin{pmatrix} \delta_f \\ \delta_r \\ \delta_b \\ \delta_l \end{pmatrix} \qquad \textbf{Equation 3.3-7}$$

Control Forces and Torques will be devised in subsequent section. The actual motors commands are:

$$\begin{pmatrix} \delta_f \\ \delta_r \\ \delta_b \\ \delta_l \end{pmatrix} = \mathcal{M}^{-1} \begin{pmatrix} F \\ \tau_\phi \\ \tau_\theta \\ \tau_\psi \end{pmatrix} \qquad \textbf{Equation 3.3-8}$$

In the vehicle frame f^v, the gravity force acting on the center of mass is given by:

$$f_g^v = \begin{pmatrix} 0 \\ 0 \\ mg \end{pmatrix} \qquad \textbf{Equation 3.3-9}$$

However, since v in Equation (7) is expressed in F^b, we must transform to the body frame to gives:

$$f_g^b = R_v^b \begin{pmatrix} 0 \\ 0 \\ mg \end{pmatrix}$$

$$= \begin{pmatrix} -mg\sin\theta \\ mg\cos\theta\sin\phi \\ mg\cos\theta\cos\phi \end{pmatrix} \qquad \textbf{Equation 3.3-10}$$

Therefore, Kinematic and Dynamic equations can be rewritten as follows:

$$\frac{d}{dt} \begin{pmatrix} p_n \\ p_e \\ h \end{pmatrix} = \begin{bmatrix} c_\psi c_\theta & s_\phi s_\theta c_\psi - c_\phi s_\psi & c_\phi s_\theta c_\psi + s_\phi s_\varphi \\ c_\theta s_\psi & s_\phi s_\theta s_\psi + c_\psi c_\phi & c_\phi s_\theta c_\psi - c_\psi s_\phi \\ s_\theta & -c_\theta s_\phi & -c_\theta c_\phi \end{bmatrix} \begin{pmatrix} u \\ v \\ w \end{pmatrix} \qquad \textbf{Equation 3.3-11}$$

$$\begin{pmatrix} \dot{u} \\ \dot{v} \\ \dot{w} \end{pmatrix} = \begin{pmatrix} rv - qw \\ pw - ru \\ qu - pv \end{pmatrix} + \begin{pmatrix} -g\sin\theta \\ g\cos\theta\sin\phi \\ g\cos\theta\cos\phi \end{pmatrix} + \frac{1}{m} \begin{pmatrix} 0 \\ 0 \\ -F \end{pmatrix} \qquad \textbf{Equation 3.3-12}$$

$$\begin{pmatrix} \dot{\phi} \\ \dot{\theta} \\ \dot{\varphi} \end{pmatrix} = \begin{pmatrix} 1 & \sin\phi\tan\theta & \cos\phi\tan\theta \\ 0 & \cos\phi & -\sin\phi \\ 0 & \frac{\sin\phi}{\cos\theta} & \frac{\cos\phi}{\cos\theta} \end{pmatrix} \begin{pmatrix} p \\ q \\ r \end{pmatrix} \qquad \textbf{Equation 3.3-13}$$

$$\begin{pmatrix} \dot{p} \\ \dot{q} \\ \dot{r} \end{pmatrix} = \begin{pmatrix} \dfrac{J_y - J_z}{J_x} qr \\[2ex] \dfrac{J_z - J_x}{J_y} pr \\[2ex] \dfrac{J_x - J_y}{J_z} pq \end{pmatrix} + \begin{pmatrix} \dfrac{1}{J_x} \tau_\emptyset \\[2ex] \dfrac{1}{J_y} \tau_\theta \\[2ex] \dfrac{1}{J_z} \tau_\psi \end{pmatrix}$$

Equation 3.3-14

Chapter 4

Control Forces and Torques

The model developed in chapter 2 describes the differential equations of the system. Hub forces and rolling moments are neglected and thrust and drag coefficients are supposed constant. The translated motor control signal U which is dependent on the square of angular speeds of the rotors is given as follows:

$$U = [U_1 U_2 U_3 \ U_4]$$

$$U_1 = [b(\Omega_1^2 + \Omega_2^2 + \Omega_3^2 + \Omega_4^2)]$$

$$U_2 = [b(-\Omega_2^2 + \Omega_4^2)]$$

$$U_3 = [b(\Omega_1^2 - \Omega_3^2)]$$

$$U_4 = [d(-\Omega_1^2 + \Omega_2^2 - \Omega_3^2 + \Omega_4^2)]$$

Where U_1 is the Altitude Control command, U_2 is the Rolling command, U_3 is Pitching command and U_4 is the Yawing command.

4.1. Rotor Dynamics

Actuators are four fixed-pitch rotors; each one includes a Brush-Less Direct Current (BLDC) motor, a one-stage gearbox and a propeller. A first-order transfer function is sufficient to reproduce the dynamics between the propeller's speed set-point and its true speed. [5]

$$G(s) = \frac{0.936}{0.178s+1} \qquad \text{Equation 4.1-1}$$

A sensor-less BLDC motors require a minimum speed to run thus, the set-point does not start from zero therefore a non-unity gain as shown in transfer function's numerator validates our rotor model.

4.2. PD control

The dynamic model (3.1-6) presented above contains two gyroscopic effects. The influence of these effects in our case is less important than the motor's action; especially if we consider a near-hover situation. In order to make it possible to design multiple PD

controllers for this system, one can neglect these gyroscopic effects and thus remove the cross coupling.

$$I_{xx}\ddot{\emptyset} = lU_2$$

$$I_{yy}\ddot{\theta} = lU_3$$

$$I_{xx}\ddot{\psi} = U_4$$

If we include in (4.1-1), the rotor dynamics and rewrite the model in Laplace domain we obtain:

$$\emptyset(s) = \frac{B^2 bl}{s^2(s + A^2)I_{xx}}(u_4^2(s) - u_2^2(s))$$

$$\theta(s) = \frac{B^2 bl}{s^2(s + A^2)I_{yy}}(u_3^2(s) - u_1^2(s))$$

$$\psi(s) = \frac{B^2 d}{s^2(s + A^2)I_{zz}}((-1^{i+1})\sum_{i=1}^{4} u_2^2(s))$$

where A and B are the coefficients of the linearized rotor dynamics, while C, too small comparing to B, is neglected. By using the control inputs U_i instead of the motor inputs u_i, above equation becomes:

$$\emptyset(s) = \frac{A^2 l}{s^2(s + A^2)I_{xx}}(U_2)$$

$$\theta(s) = \frac{A^2 l}{s^2(s + A^2)I_{yy}}(U_3)$$

$$\psi(s) = \frac{A^2}{s^2(s + A^2)I_{zz}}(U_4)$$

The numerical application gives:

$$\emptyset(s) = \frac{0.522}{0.004s^4 + 0.039s^3 + 0.009s^2}(U_2)$$

$$\theta(s) = \frac{0.522}{0.004s^4 + 0.039s^3 + 0.009s^2}(U_3)$$

$$\psi(s) = \frac{21.78}{0.008s^4 + 0.077s^3 + 0.18s^2}(U_4)$$

A PD controller is introduced for each orientation angle:

$$U_{2,3,4} = k_{\emptyset,\theta,\psi}(\emptyset, \theta, \psi) + d_{\emptyset,\theta,\psi}(\emptyset, \theta, \psi)$$

Several simulations were performed on Simulink using the complete model in order to tune the six control parameters. The controller's task was to stabilize the orientation

angles. For these simulations, the Dynamic model (18) was used, obtaining the results shown in Fig. 4.2.1. The simulated performance was satisfactory regarding the simple control synthesis approach.
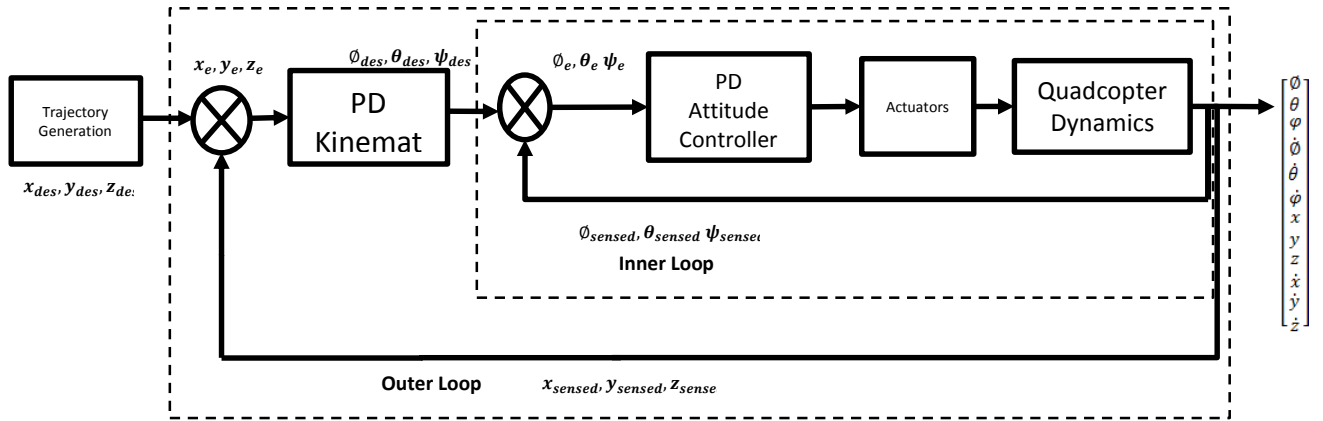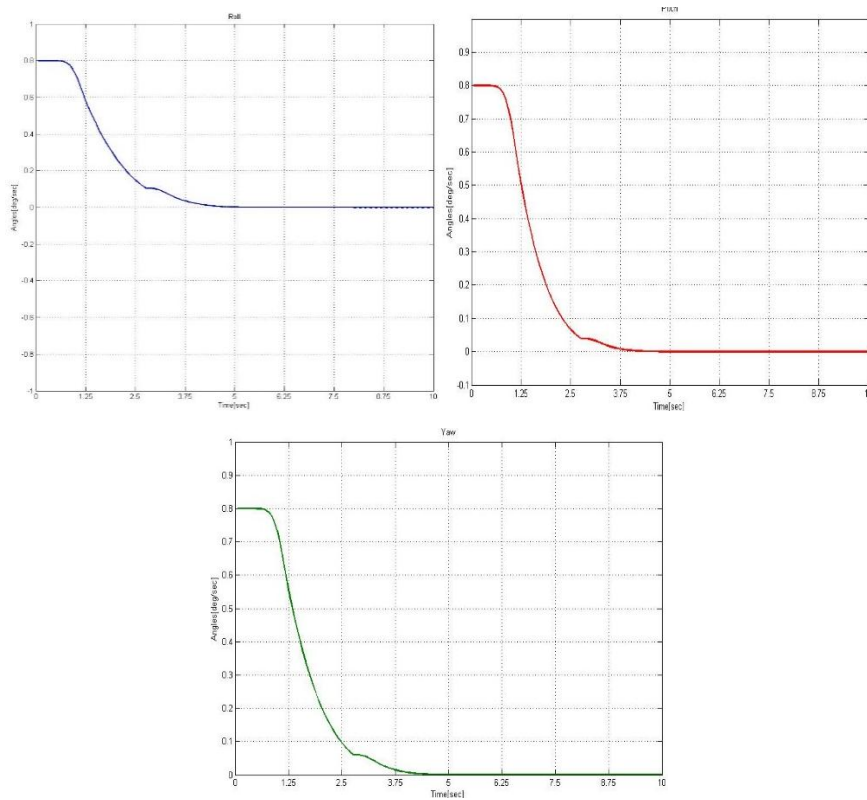

Figure 4.2-1 PD Control Loop

Figure 4.2-2 Roll, Pitch and Yaw Results with Initial Conditions

4.3. Fuzzy Adaptive Control

4.3.1. Generalized Fuzzy Control Scheme

Fuzzy control technique is comparatively new in which input variables are mapped onto membership function this process is called fuzzification and the membership values quantify the implication degree of a rule from rule base. On the basis of rule base a conclusion is made using inference mechanism in the end defuzzification converts membership values into crisp output. [12]

Generalized fuzzy control system is given below:
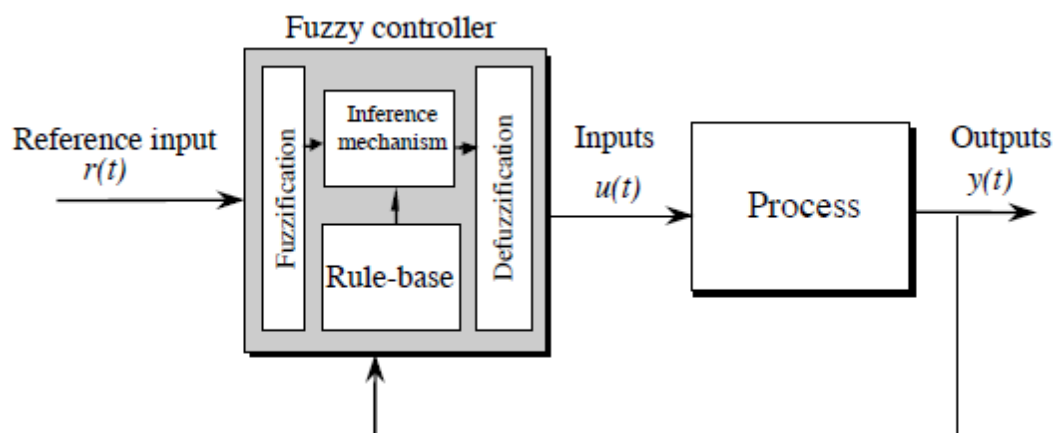
Figure 4.3.1-1 Fuzzy PD Control Loop

4.3.2. Fuzzy Gain Scheduled PD Control
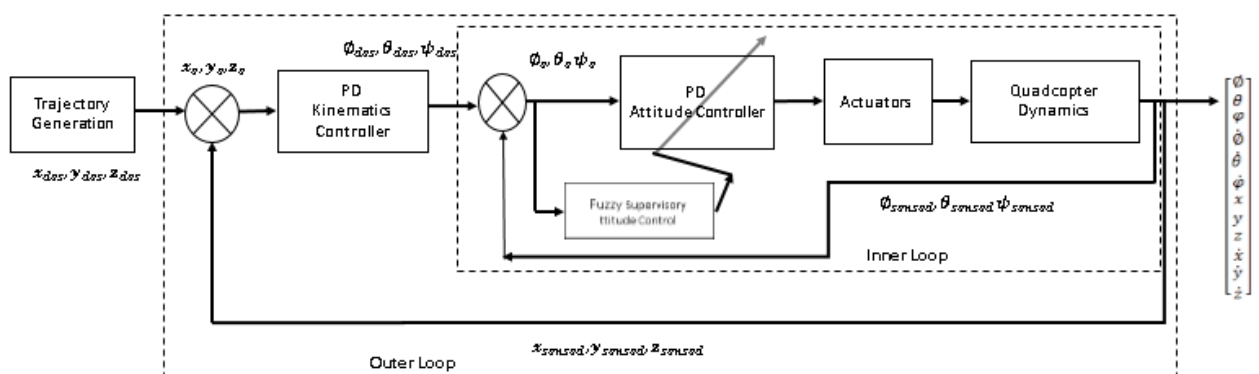
Figure 4.3.2-1 Fuzzy PD Control Loop

The transfer function of a conventional PD controller is:

$$G(s) = K_p + \frac{K_d}{s}$$ Equation 4.3.2-1

where K_p and K_d are the proportional and derivative gains, respectively. A Takagi-Sugeno (TS) type Fuzzy Logic Controller (FLC) tunes the PD gains online where the tracking error 'e' and the change of the tracking error 'edot' are used to determine control parameters. Linear transformation gives the modified controller gains as follows [10] [8]:

$$K_p = \left(K_{p,max} - K_{p,min}\right)K_p' + K_{p,min} \qquad \text{Equation 4.3.2-2}$$

$$K_d = \left(K_{d,max} - K_{d,min}\right)K_d' + K_{,min} \qquad \text{Equation 4.3.2-3}$$

with $[K_{p,min}; K_{p,max}]$ and $[K_{d,min}; K_{d,max}]$ are pre-determined ranges of K_p, and K_d respectively.[9]

4.3.3. Takagi-Sugeno Type Fuzzy Inference

The type of Fuzzy Controllers used in this research is are based on Takagi-Sugeno (TS) type fuzzy inference mechanism.

A typical rule in a Sugeno fuzzy model has the form:

If Input 1 = x and Input 2 = y, then Output is z = ax + by + c

Instead of a membership function at the output (as in Mamdani) there is a linear equation or a singleton. [12]

This gives an edge over a resource hungry Mamdani fuzzy inference mechanism since there are no output membership function so there is a less memory requirement and thus the control activity is much limited yet very precise.

A set of linguistic rules used in the FLC structure determine K_p' and K_d'. The If-Else set of linguistic rules are derived from expert knowledge essentially on the basis of Open loop manual control.

Rule statements comprise of an Antecedent and Consequence as following example demonstrates: [10]

- If e is Negative Big (N. B) and $\dot{e}$ is Negative Big (N.B) than μ_{con} is Positive Big (N.B).
- If e is Negative Small (N. S) and $\dot{e}$ is Negative Big (N.B) than μ_{con} is Positive Big (N.B); and so on.

$\mu_e \mid \mu_{\dot{e}}$	NB	NM	NS	Z	PS	PM	PL
N.B	B	B	B	B	B	B	B
N.M	S	B	B	B	B	B	S

N.S	S	S	B	B	B	S	S
Z	S	S	S	B	S	S	S
P.S	S	S	B	B	B	S	S
P.M	S	B	B	B	B	B	S
P.B	B	B	B	B	B	B	B

Table 4.3.3-1 Fuzzy PD If-Else Rules for K$_p$

$\mu_e \backslash \mu_{\dot{e}}$	NB	NM	NS	Z	PS	PM	PL
N.B	B	B	B	B	B	B	B
N.M	M	M	B	B	B	M	M
N.S	S	M	M	B	M	M	S
Z	Z	S	M	B	M	S	Z
P.S	S	M	M	B	M	M	S
P.M	M	M	B	B	B	M	M
P.B	B	B	B	B	B	B	B

Table 4.3.3-2 Fuzzy PD If-Else Rules for K$_d$
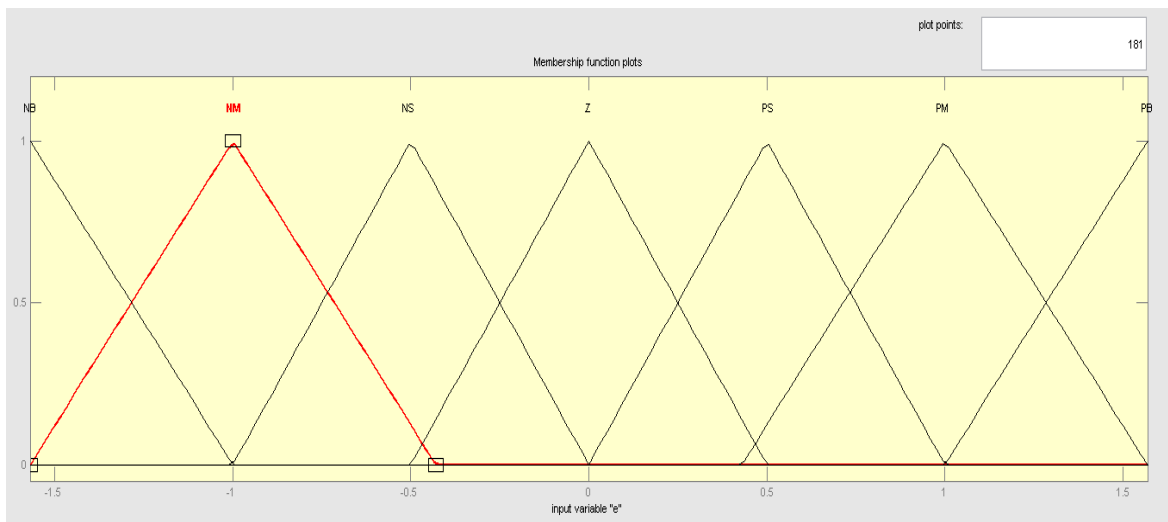
Figure 4.3.3-1 Membership Functions for tracking error 'e'
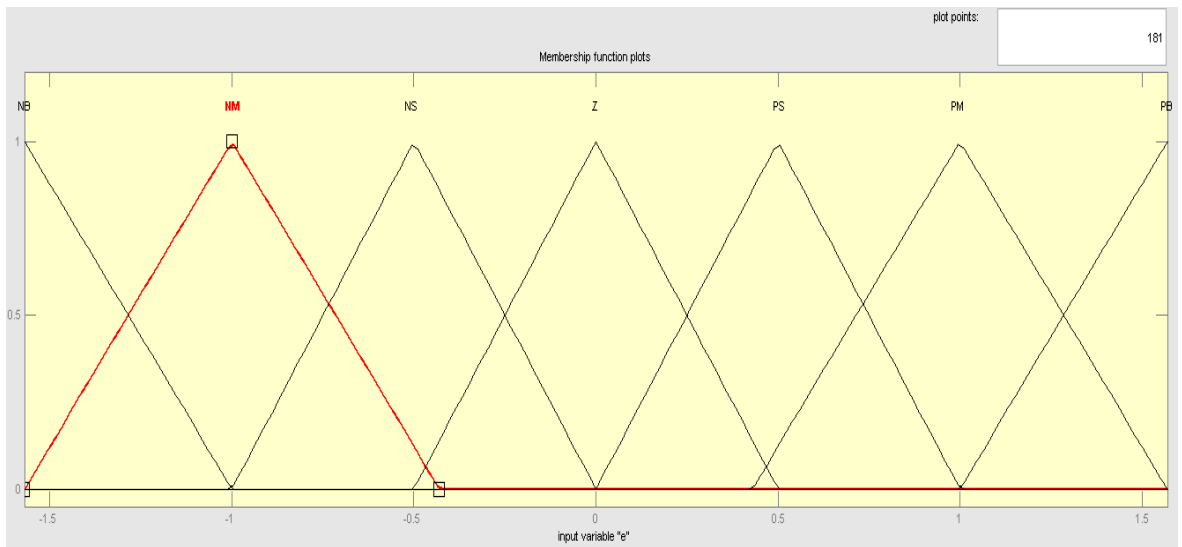
Figure 4.3.3-2 Membership Functions for tracking error derivative 'edot'
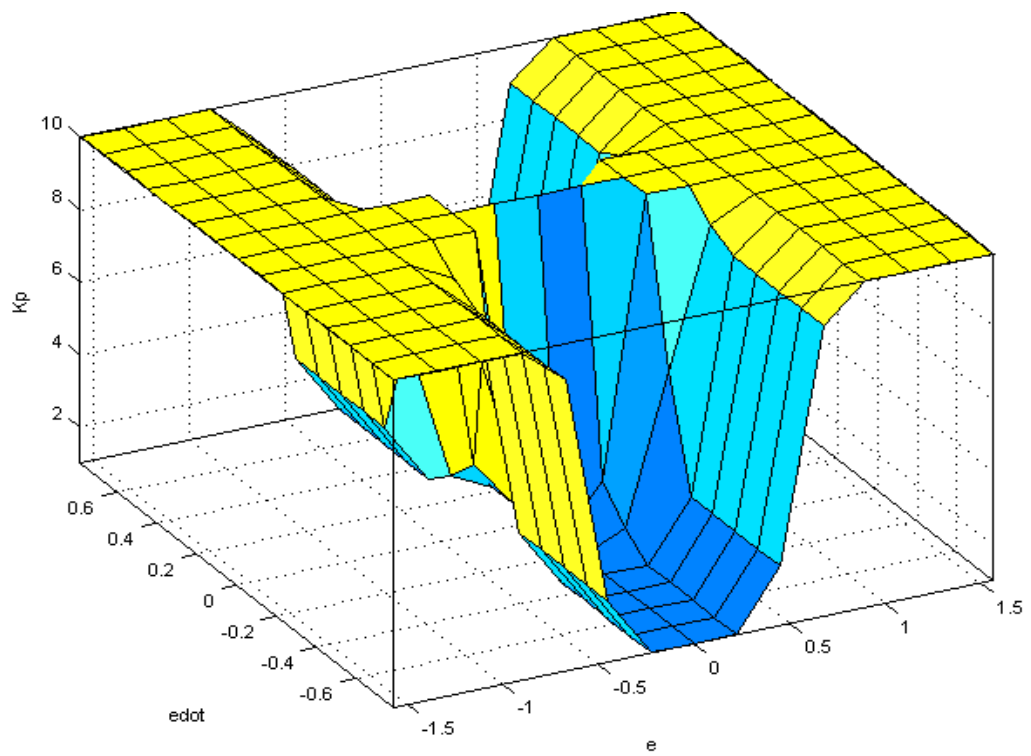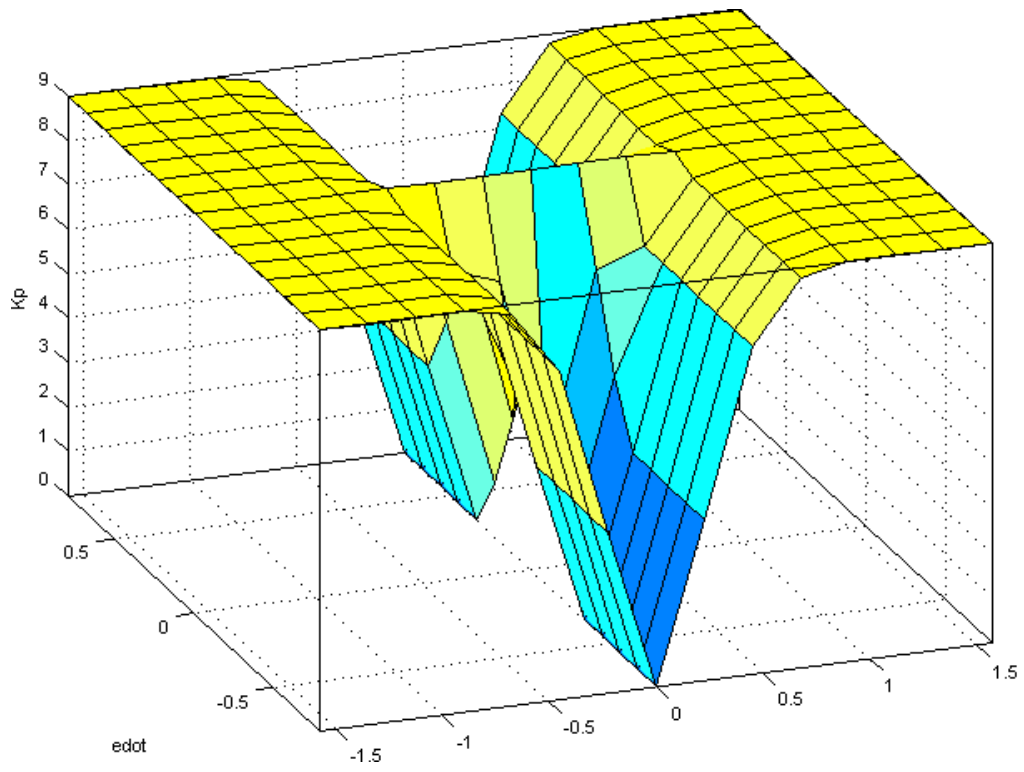
Figure 4.3.3-3 Control Surfaces for Kp and Kd respectively based on Fuzzy rules

Chapter 5

Results and Simulations

In this section attitude and trajectory control simulations of Quadcopter will be discussed. Simulations were performed in Matlab/ Simulink by employing the highly realistic model of 6 DoF equations [6 and 8] of motion derived in chapter above. First these real-time simulations were performed by implementing PD control strategy than on the same model Fuzzy GS PD Controller was implemented and the comparisons between both results are given at the end of this chapter. [11]

In Simulink Matlab simulation, a complete Non-Linear 6-DoF Coupled model of Quadcopter was implemented and subjected to the tests with both PD and Fuzzy GS PD Controllers. Real-Time simulation was performed using Matlab and Simulink. During the design of PD control scheme it was made sure that all the stated were observable since PD would only work if all states are available at the Output. Following quadcopter constants were assumed for the simulations.

S.no	Parameter	Value	Unit
1	Gravitational acceleration (g)	9.8	m/s^2
2	Mass of Quadcopter (m)	1	Kg
3	Length of wings (l)	0.24	m
4	Rotational Inertia along x-axis (J_x)	8.1×10^{-3}	Kg.m^2
5	Rotational Inertia along y-axis (J_y)	8.1×10^{-3}	Kg.m^2
6	Rotational Inertia along z-axis (J_z)	14.2×10^{-3}	Kg.m^2
7	Residual Rotational Inertia (J_r)	104×10^6	Kg.m^2
8	Initial Roll, Pitch and Yaw Angles	[0.8;0.8;0.8]	degrees
9	Motor constant (K_e)	6.2×10^{-3}	-
10	Motor constant (K_m)	6.2×10^{-3}	-
11	Drag Factor	1.1×10^{-6}	-

Table 0-1 Quadcopter Physical/Simulated Constants

The trajectory generation block simulates vertical takeoff/landing, hover and moving to a desired 3 dimensional space. At the end of each maneuver a quadcopter's attitude angles should settle to zero i.e. hover at a point as seen in the figures 17 and 23. It is seen in the Simulink model [figure 12] the model that converts control constants $[U_{roll}, U_{pitch}, U_{yaw}]$ to motor control signals $[U_1, U_2, U_3, U_4]$ also known as ESC (Electronic Speed Converter) that generates a corresponding PWM signal for Motor speed control [7]. Motors are represented by four first order transfer functions. The

quadcopter dynamics block contains the 6 DoF dynamics equations of motion. The accelerations are obtained at the end of the dynamics block which are then integrated to obtain rotational as well the translational velocities and (linear and angular) positions.

5.1. Simulation with Simple PD control strategy

Initial conditions for all state variables are set to zero. Measurement Noise block is inducing sensor noise in the system to make simulations more realistic. PD control parameters are presented in below table. [9]

Variable	Parameter Value		
i	$K_{i,p}$	$K_{i,d}$	$K_{i,i}$
x	5	10	-
y	5	10	-
z	5	10	-
$\emptyset$	10	20	-
θ	10	20	-
φ	10	20	-
Motor	1	-	10

Table 5.1-1 PD Gains
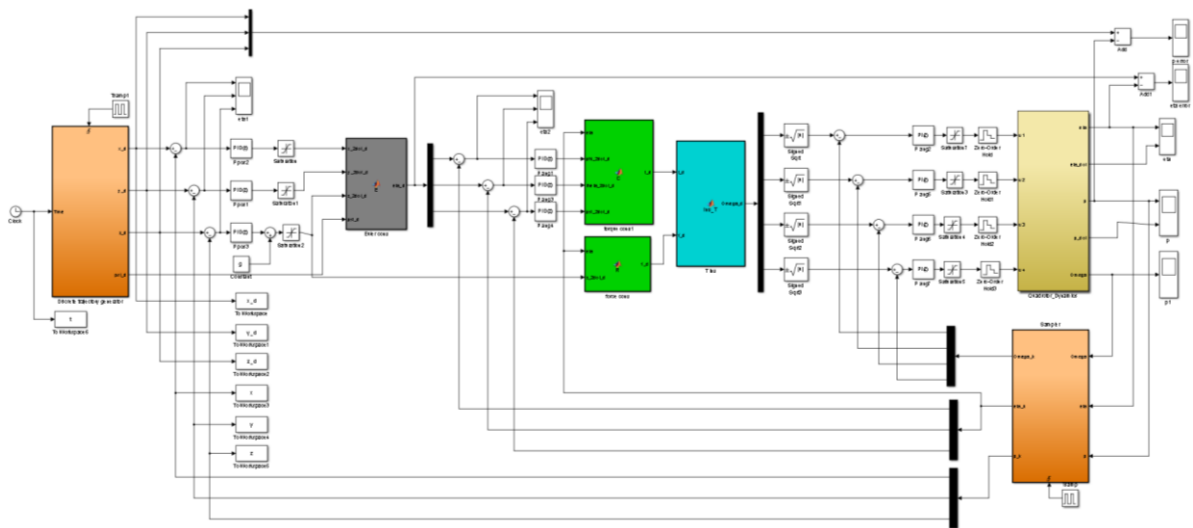
Figure 5.1-1 Simulink Model of Real Time simulation with PD Controller

5.1.1. Simulation Results

Simulation results are obtained for period of 100 sec. It is clearly observed in figure 15 there is a considerable steady state error and the quadcopter is constantly trying to adjust its attitude to make adjustments for the wind flowing over its propellers which due to fixed PD gains can't change or vary according to changing speed of wind.
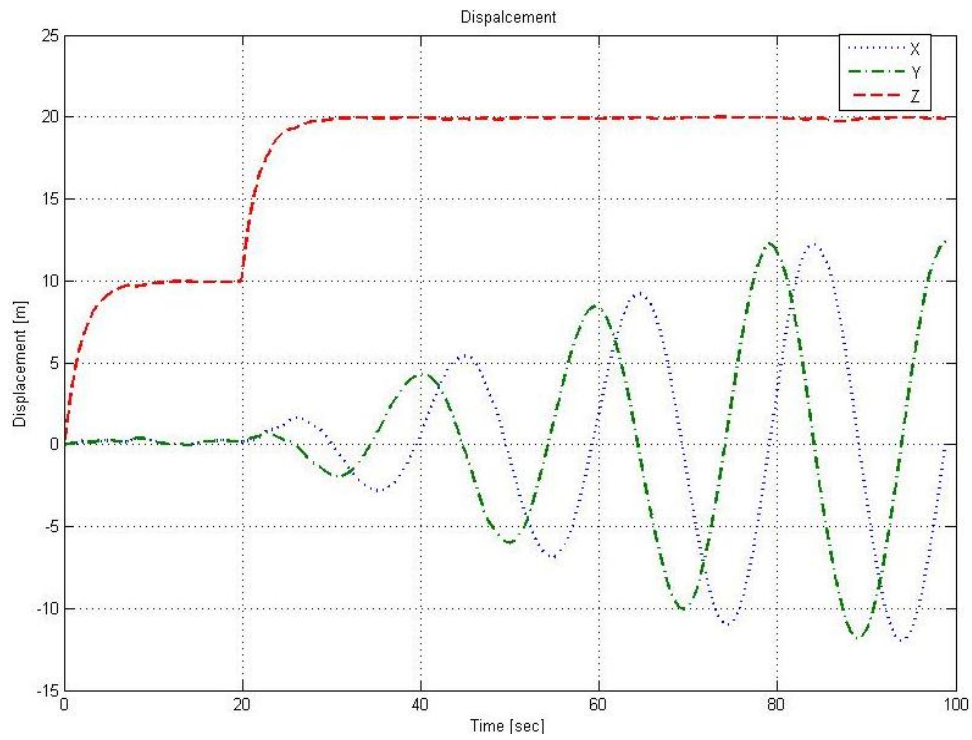
Figure 5.1.1-1 Displacement Results with PD Controller
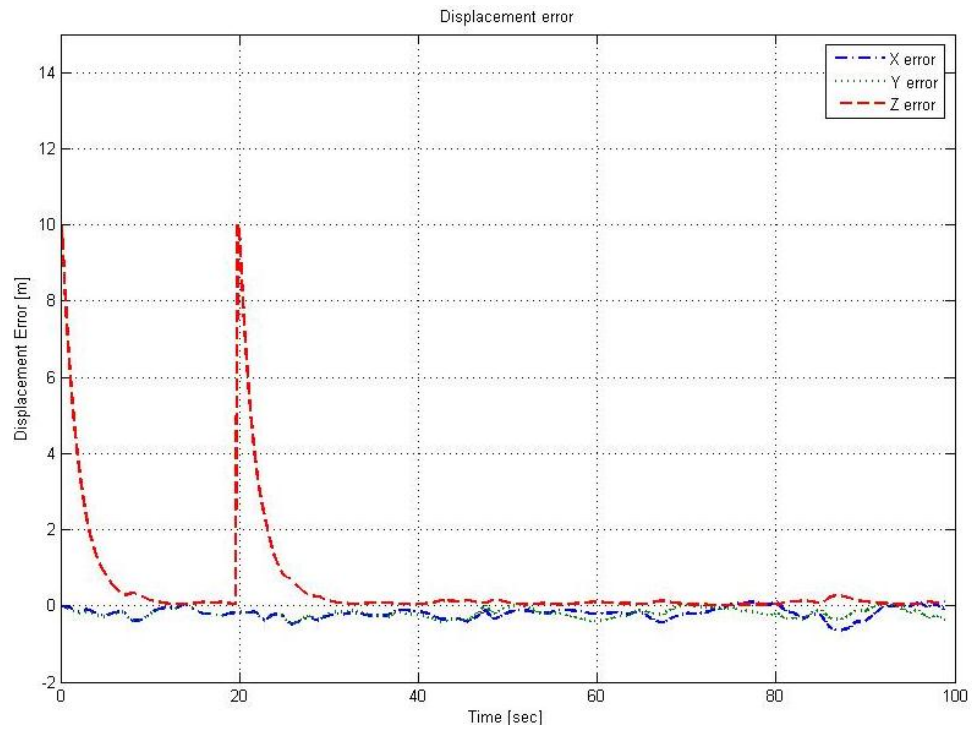
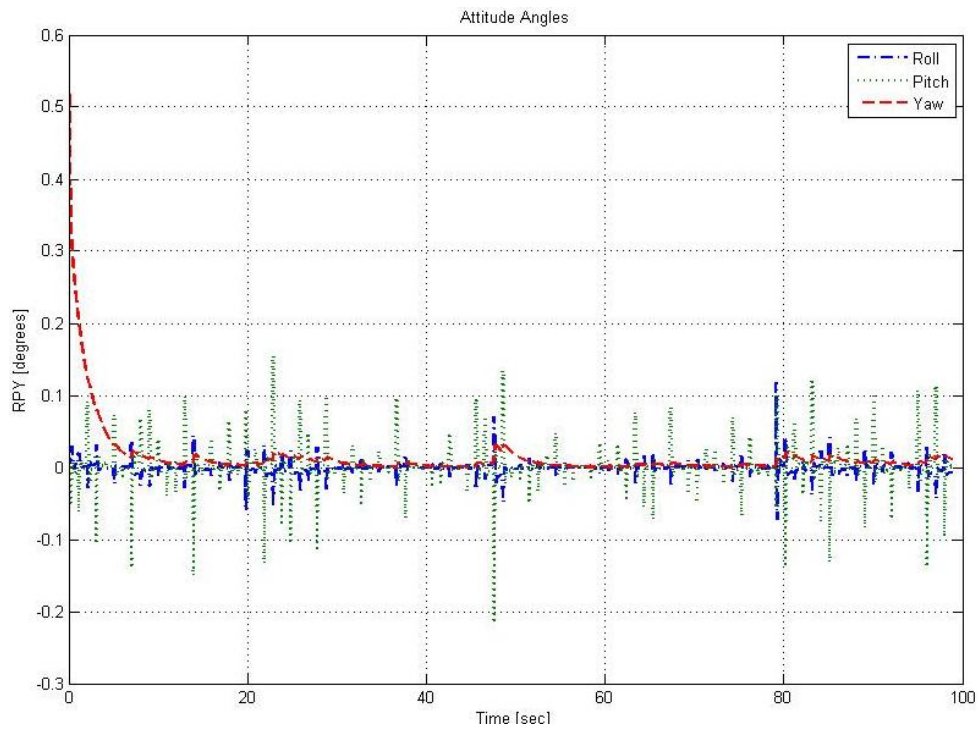
Figure 5.1.1-2 Displacement error Results with PD Controller
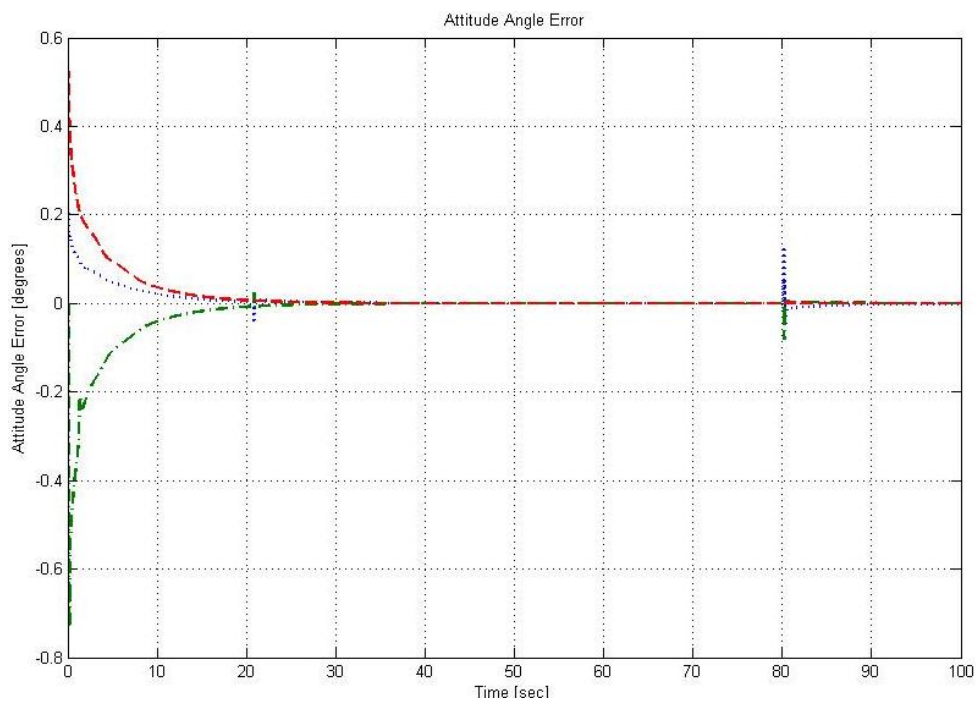
Figure 5.1.1-3 Attitude Angles with PD Controller

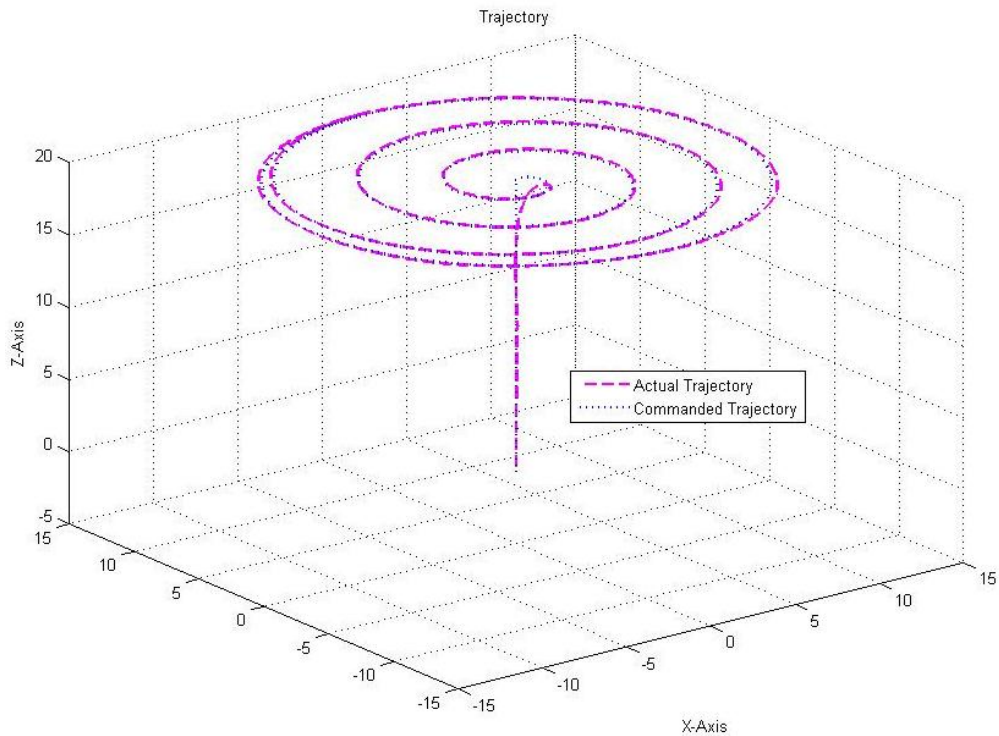**Figure 5.1.1-4 Attitude Angles error with PD Controller**

34

Figure 5.1.1-5 Trajectory Following with PD Controller

5.2. Simulation with Self Tuning Fuzzy PD control strategy

Following the similar procedure as described in 5.1; a Fuzzy GS PD Control scheme was also simulated to verify their performance. Same quadcopter constants were used along with the similar 6 DoF dynamic model.

Almost everything is similar except Fuzzy GS PD controller block. Furthermore, same scaling is ensured for the same type of results with different control scheme where possible.
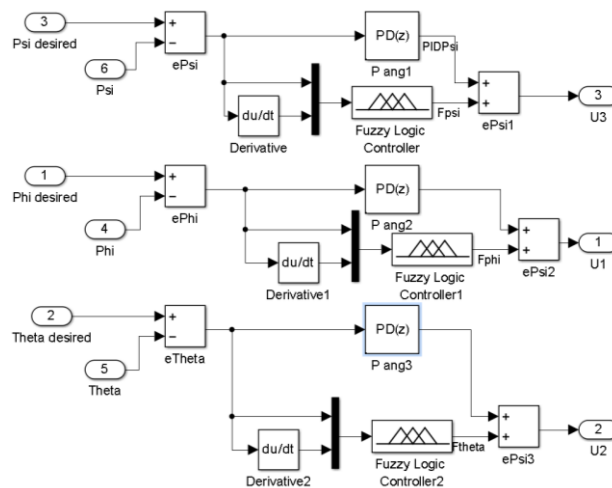
Figure 5.2-1 Simulink Model for Fuzzy PD Controller

5.2.1. Simulation Results

Simulation results are obtained for period of 100 sec. It is clearly observed in figure 5.2.1-1 there is no steady state error and the quadcopter is smoothly flying even in simulated gusty environment.
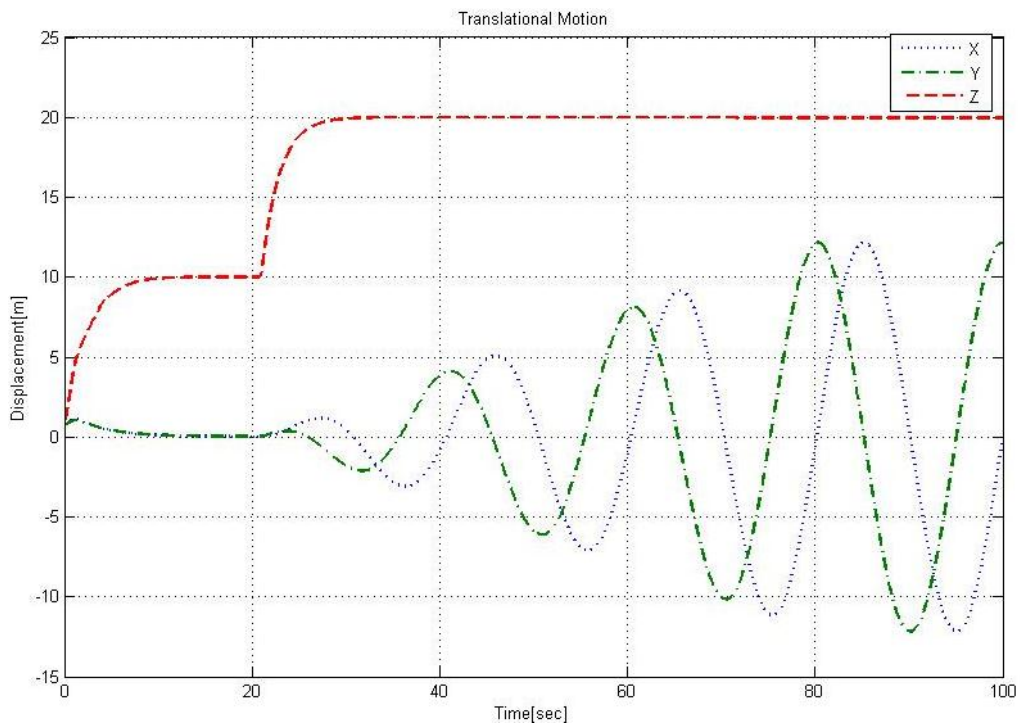
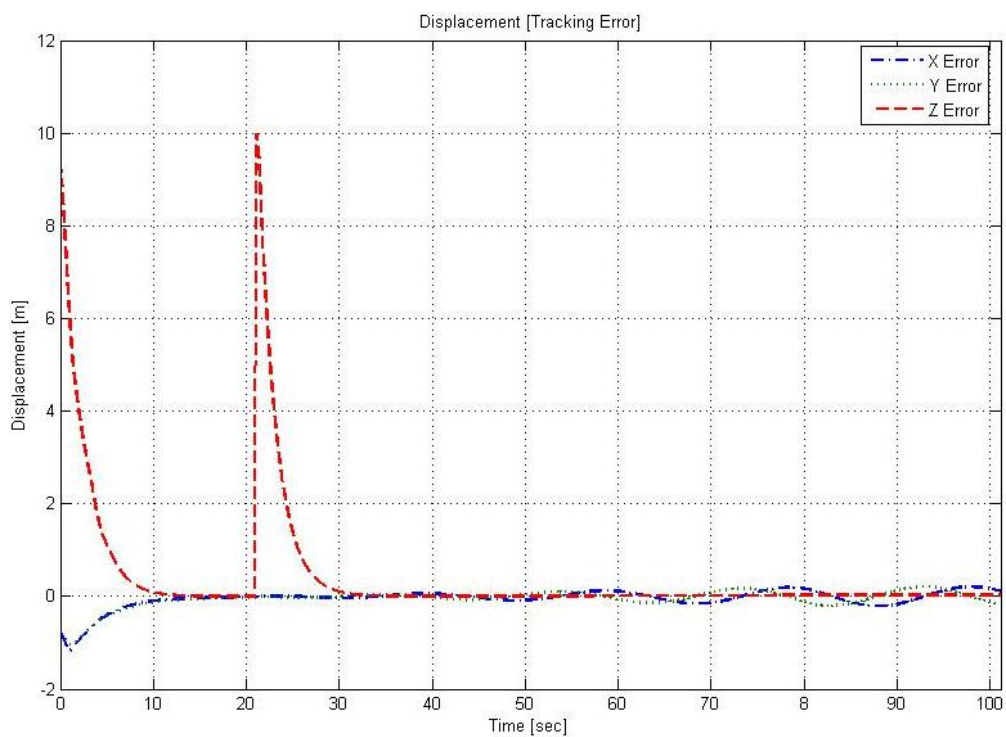
Figure 5.2.1-2 Displacement
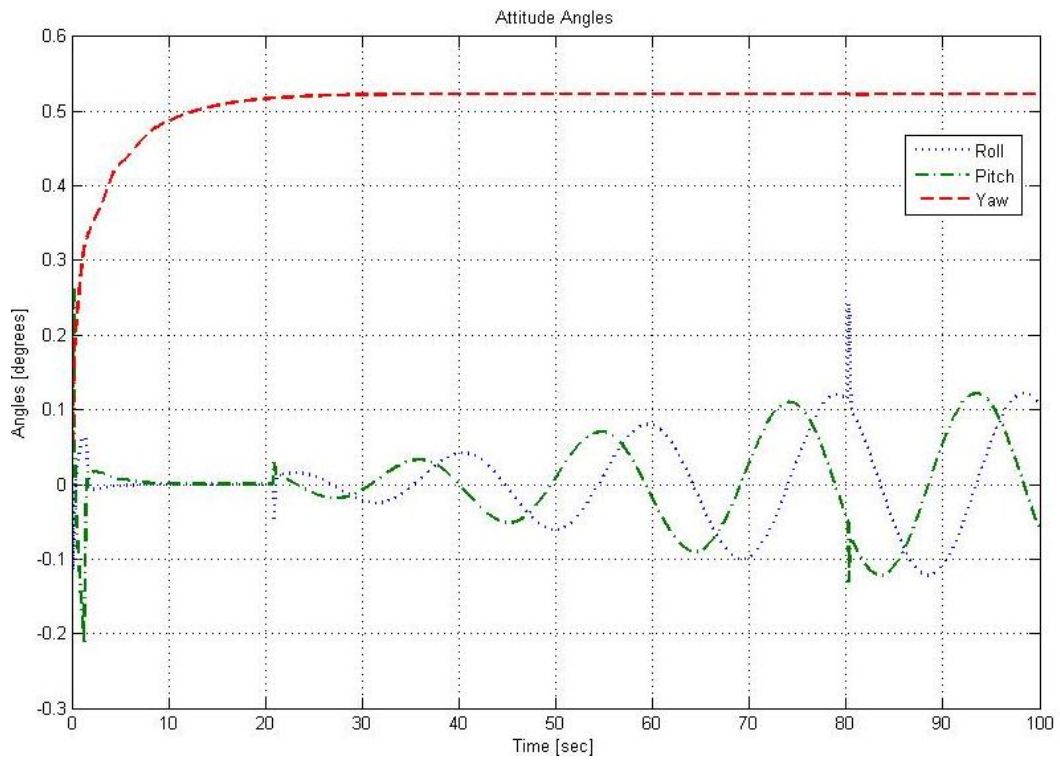
Figure 5.2.1-3 Displacement Error

Figure 5.2.1-4 Attitude Angles [Roll, Pitch, Yaw]
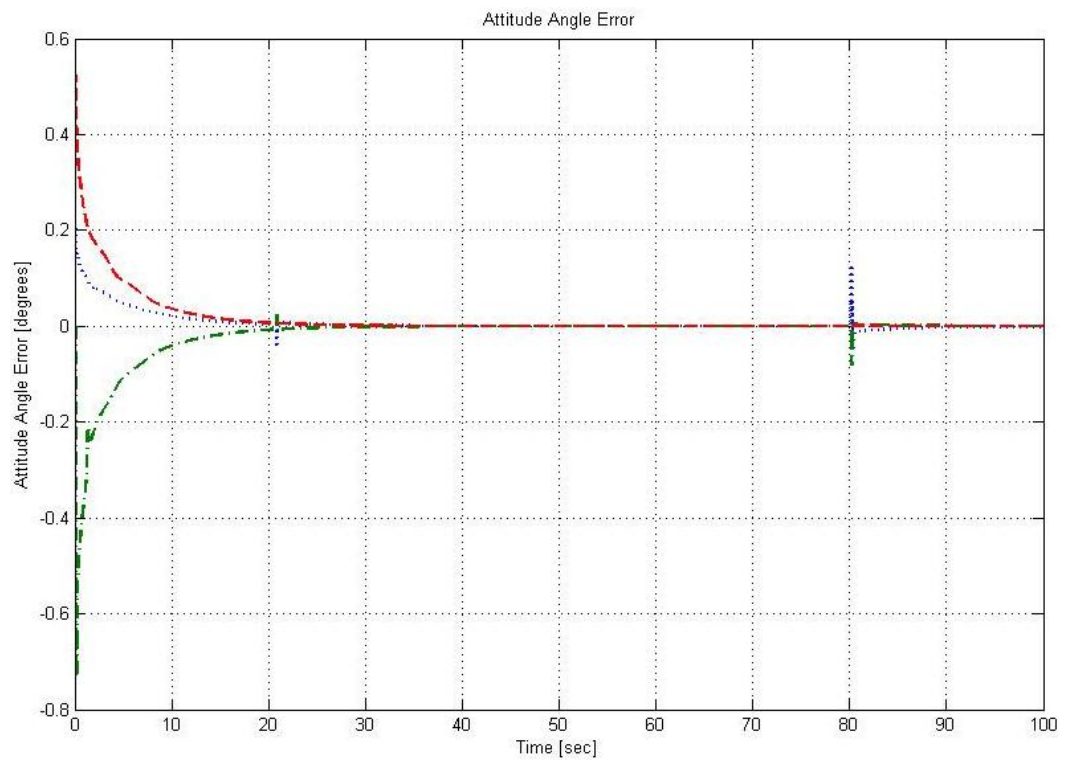
Figure 5.2.1-5 Angle Error
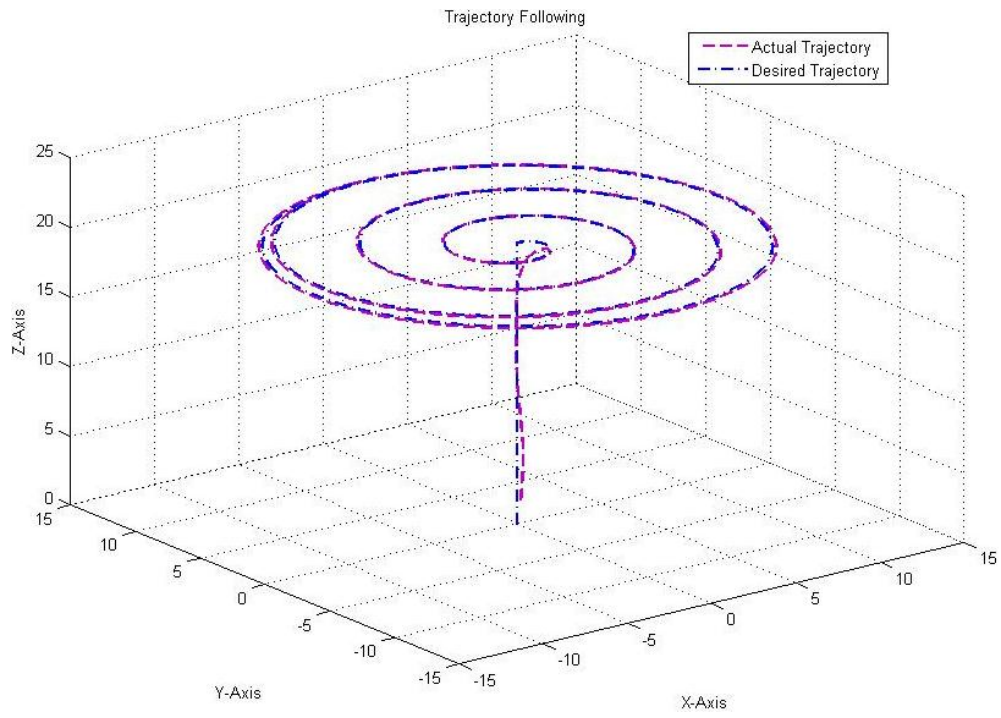
Figure 5.2.1-6 Trajectory Results

The RMSE results are compared for a Step Input actuated at different time intervals for x, y and z in order to generate 3-axes maneuvers along with hovers.
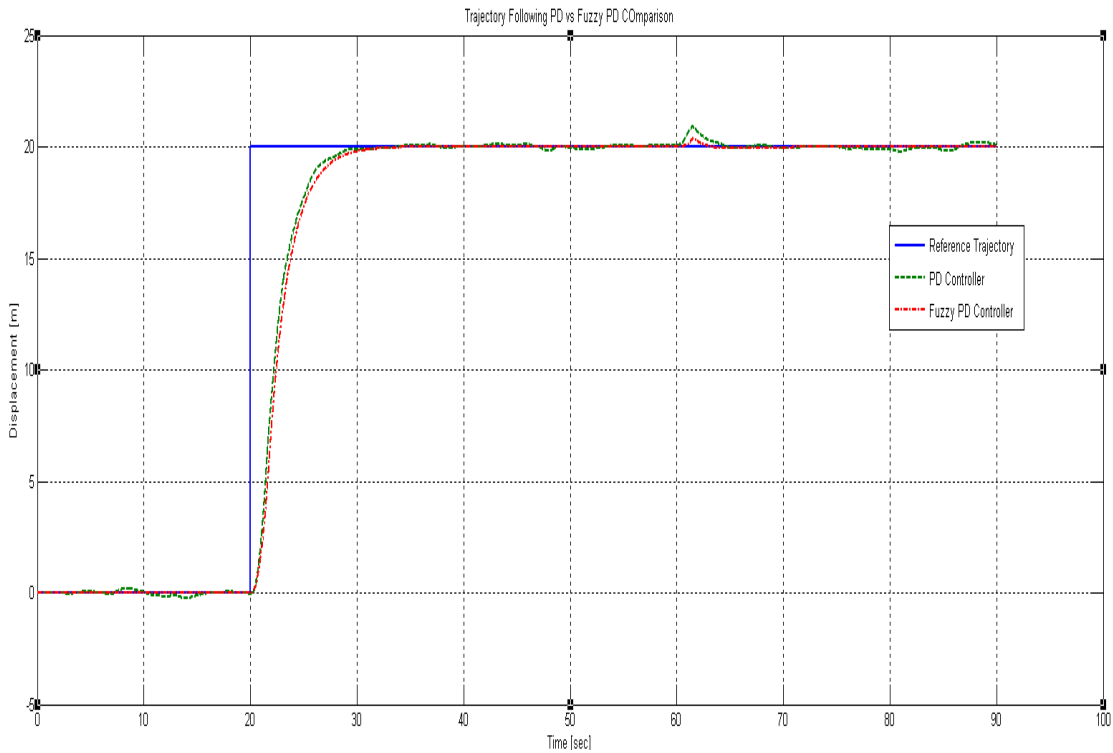
5.2.2. Movement and Hover along X-Axis

Figure 5.2.2-1 Trajectory Results for X Axis

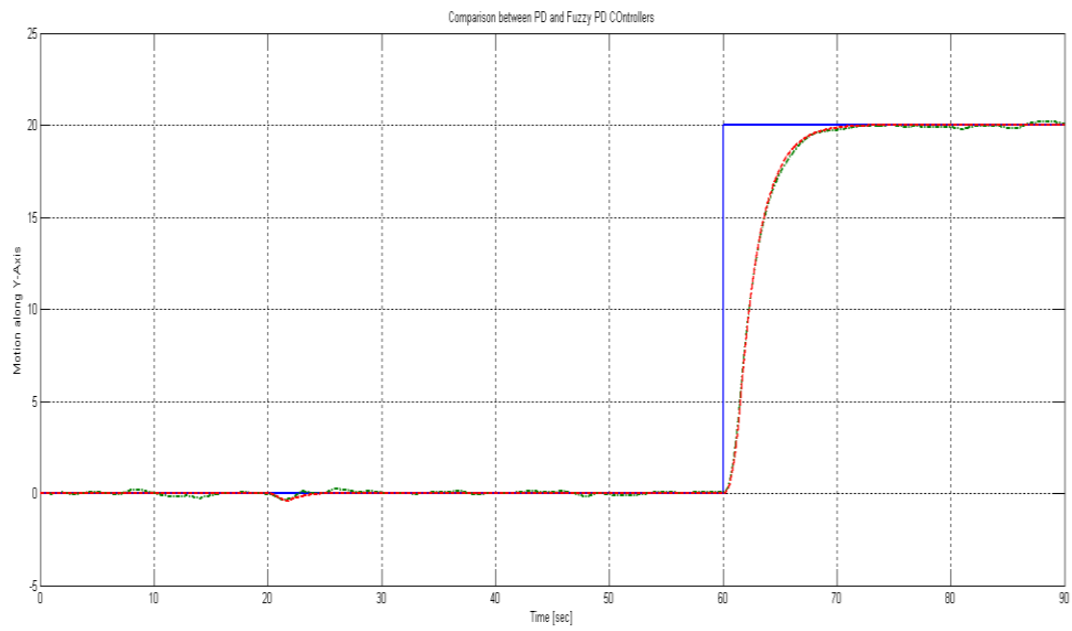## 5.2.3. Movement and Hover along Y-Axis

Figure 5.2.3-1 Trajectory Results for Y Axis
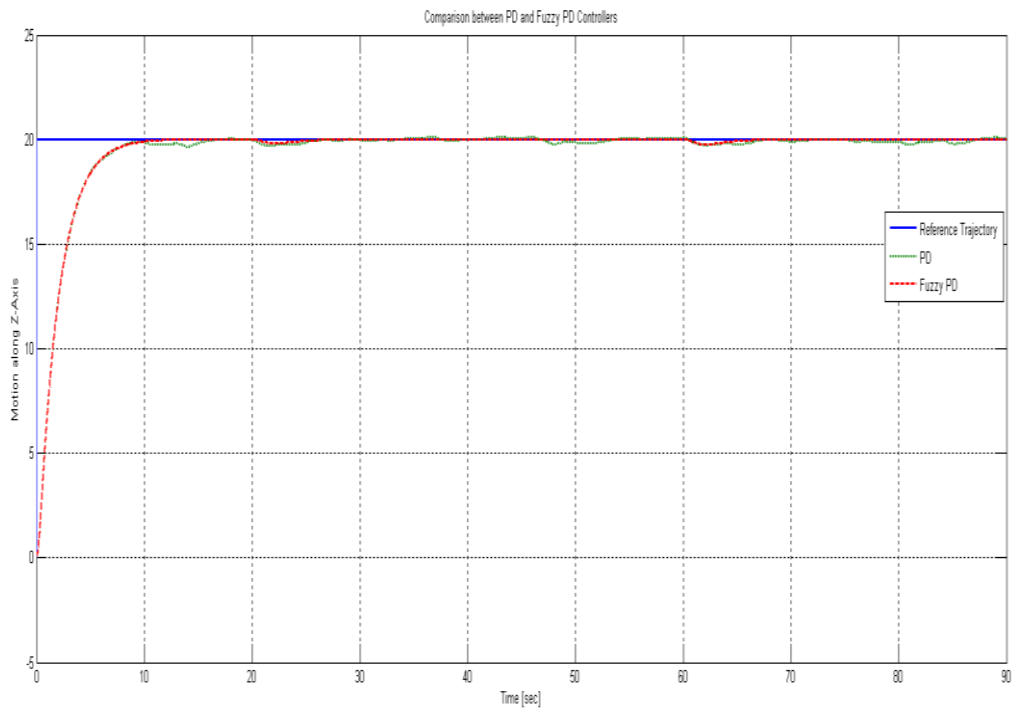
5.2.4. Movement and Hover along Z-Axis

Figure 5.2.4-1 Trajectory Results for Z Axis

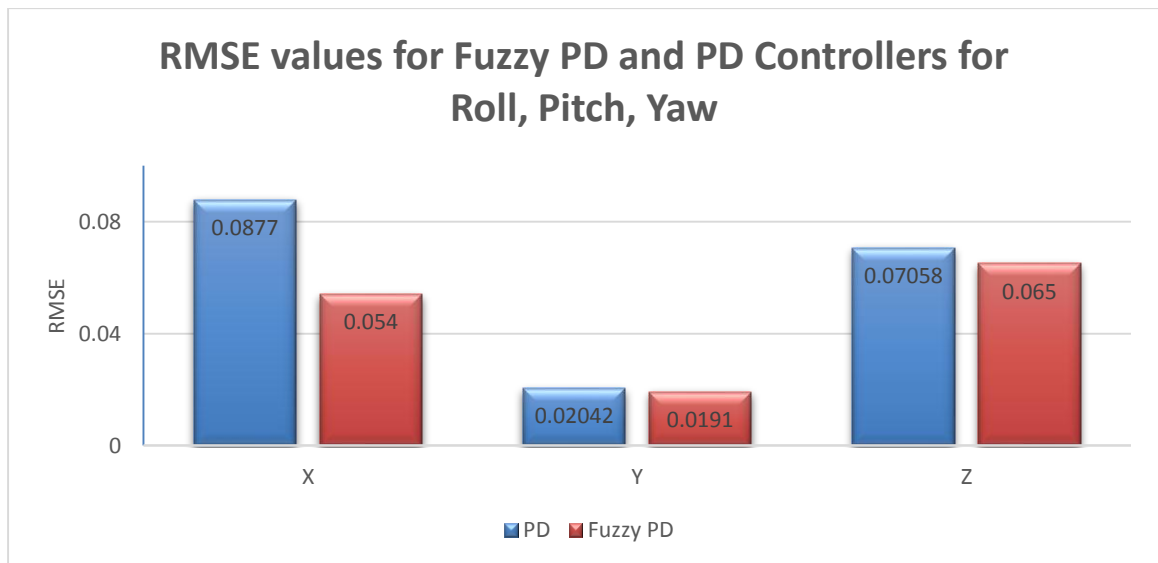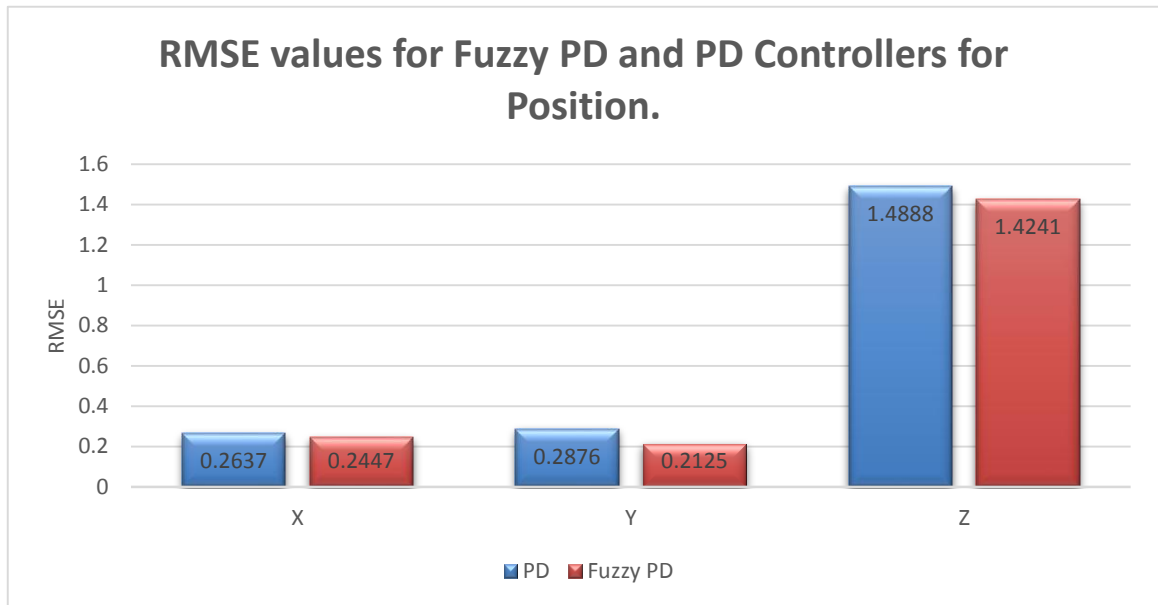Figure 5.2.4-2 RMSE Results for Motion along x, y and z axes

Figure 5.2.4-3 RMSE Results for Rotational Motion

It is clear that the PD controller cannot coupe up with the Disturbances resulting in a Non-Smooth Tracking and increased control activity which would ultimately damage the Motors.

Chapter 6

Conclusion

This thesis addressed the design of a Realistic and highly Non-Linear coupled Simulator for a certain Quadcopter. The control strategy discussed is a fuzzy gain-scheduled PD controller in the presence of actuator atmospheric disturbances. The obtained simulation results revealed the effectiveness of the proposed method and its ability to adapt in the presence of uncertainties and external disturbances.

As it is clear from the results above that the fixed gain PD controller can't cope with the Real environmental disturbances like wind gusts or Ground Effect and since it can't make necessary adjustments to counter such effects there would be a significant loss in its battery consumption as the quad would make very frequent attitude adjustments with constant rotor speeds whereas the Fuzzy GS PD controller can effectively increase or decrease its gains hence the rotor speeds to counter changing disturbance effects and save the battery life without compromising the quality of work for which it has been deployed.

References

1. Fault-tolerant fuzzy gain-scheduled PID for a quadrotor helicopter testbed in the presence of actuator faults Advances in PID Control, Volume # 2 | Part# 1

2. PID vs LQ control techniques applied to an indoor micro quadrotor S. Bouabdallah, A. Noth, R. Siegwart Autonomous Syst. Lab., Swiss Fed. Inst. of Technol., Lausanne, Switzerland In proceeding of: Intelligent Robots and Systems, 2004. (IROS 2004). Proceedings. 2004 IEEE/RSJ International CoPIDnference on, Volume: 3 Source: IEEE Xplore

3. Fuzzy Gain Scheduling PID Control Design Based on Particle Swarm Optimization Method; *Ker-Wei*, *Yu and Jia-Hao Hsu*, Department of Marine Engineering, National Kaohsiung Marine University, 482, Jhongjhou 3rd Road, Cijin, Kaohsiung 80542, Taiwan, R.O.C.

4. Smart Self-Tuning Fuzzy PID Controller *Deepak Gautam[1] and Cheolkeun Ha[2]*, The School of Mechanical Engineering, University of Ulsan.

5. Fault-Tolerant Fuzzy Gain-Scheduled PID for a Quadrotor Helicopter Testbed in the Presence of Actuator Faults; *Mohammad Hadi Amoozgar, Abbas Chamseddine, Youmin Zhang**, Concordia University, Montreal, Quebec, Canada.

6. S. Bouabdallah et al., "Design and control of an indoor micro quadrotor," in Proc. (IEEE) International conference on Robotics and Automation

7. Design and control of quadrotors with application to autonomous flying Samir BOUABDALLAH, PhD Thesis, THÈSE NO 3727 (2007) ÉCOLE POLYTECHNIQUE FÉDÉRALE DE LAUSAN

8. Zulfatman and Rahmat, M.F. (2009). Application of self-tuning fuzzy PID controller on industrial hydraulic actuator using system identification approach. Int. J. on Smart Sensing and Intelligent Systems, 2, 246-261.

9. Ziegler, J.G. and Nichols, N.B. (1942). Optimum settings for automatic controllers. ASME Trans., (64), 759-768.

10. Zhao, Z., Tomizuka, M., and Isaka, S. (1993). Fuzzy gain scheduling of PID controllers. IEEE Transactions on Systems, Man, and Cybernetics, 23(5), 1392-1398.

11. Ng, T.C.T., Leung, F.H.F., and Tam, P.K.S. (1997). A simple gain scheduled PID controller with stability consideration based on a grid-point concept. In Proceed- ings of the IEEE International Symposium on Industrial Electronics, 1090{1094. Guimaraes, Portugal.

12. MATLAB Help